Effect of Nanosized Carbon Black on the Morphology, Transport, and Mechanical Properties of Rubbery Epoxy and Silicone Composites

Mohsin Ali Raza,[1] Aidan Westwood,[1] Chris Stirling,[2] Rik Brydson,[1] Nicole Hondow[1]

[1]*Institute for Materials Research, University of Leeds, Leeds LS2 9JT, United Kingdom*
[2]*Morgan AM&T, Swansea SA6 8PP, United Kingdom*

Received 27 September 2011; accepted 10 December 2011
DOI 10.1002/app.36655
Published online in Wiley Online Library (wileyonlinelibrary.com).

ABSTRACT: Three different types of nanosized carbon black (CB), Printex XE2 (CBP), Vulcan XC72, and Printex 140 U (CBU), were dispersed by mechanical mixing in rubbery epoxy (RE) and silicone to produce composites. It was found that the maximum possible loading of CB in the polymers depended on the surface area of CB. For a given loading, all three CBs produced similar improvements in the thermal conductivity of the resulting composites, but their effects on the electrical conductivity varied and ranged from insulating composites with CBU to conducting composites with CBP. CBP produced a greater improvement in the electrical conductivity than the thermal conductivity of the polymers compared to the other CBs. This was attributed to the high structure of CBP, which led to the formation of a concatenated structure within the matrix. The CB/silicone composites had a similar thermal conductivity to that of the CB/RE composites, but only the CBP/silicone composite produced at 8 wt % loading was electrically conducting. The compression and hardness properties of RE were also significantly improved with the addition of CB. However, in the case of silicone, only CBP had a considerable effect on the compression properties. © 2012 Wiley Periodicals, Inc. J Appl Polym Sci 000: 000–000, 2012

Key words: carbon black; composites; mechanical properties; morphology; thermal properties

INTRODUCTION

Conducting polymer composites have many engineering applications, such as adhesives in electronics packaging,[1] electromagnetic interference shielding,[2] electrostatic dissipation, self-regulating heating elements,[3] flexible capacitors,[4] and pressure sensors.[5–7] Conducting polymer composites have been developed by the blending of fillers, such as carbon black (CB), graphite, and silver, into polymer matrixes.[8,9]

CB is a potential filler for making adhesives for electronic packaging applications and conducting composites. CB is an elemental form of carbon that is semicrystalline in nature. It is produced by the incomplete combustion or decomposition of gaseous or liquid hydrocarbons.[10] Apart from its applications for developing conducting polymer composites, CB is used as a reinforcement in elastomers,[11] as a pigment for inks or colored plastics,[10] in plastics for providing ultraviolet radiation resistance,[12,13] in gas sensors[14] and in batteries to improve service life.[15] CB when used as a filler in polymers can provide a wide range of electrical conductivities, ranging from insulating to conducting depending on the weight percentage of CB and the nature of the polymer.[10,16] The *percolation threshold* is defined as the critical filler content at which composites undergo a transition from an insulating to a conducting material,[17] and this is an important criterion for differentiating between such composites. A composite should have an electrical conductivity of 10^{-6} S/m or greater to meet the criterion for electrostatic applications.[18] A careful look at the electrical conductivity data published in a review article[19] and in refs. [17] and [18] clearly suggests that at the percolation threshold, the electrical conductivity of composites is about 10^{-6} S/m.

CB/polymer composites have been developed by the dispersion of CB in thermoplastics, thermosetting plastics, and elastomers. For electronic packaging applications, curable thermoset polymers such as epoxies and silicones are more advantageous, as they offer ease of application and have good strength, moisture and chemical resistance, and high thermal stability. CB/epoxy composites have been developed for various applications. In particular, previous studies in the literature have concentrated on their electrical conduction behavior. These are summarized in Table I.

In contrast to the rather conventional use of CB in the development of electrically conducting polymers, CB has also been employed in thermal pastes for thermal interface applications in electronics. These

Correspondence to: M. A. Raza (mohsinengr@yahoo.com).

TABLE I
Literature Data for the CB/Epoxy and CB/Silicone Composites

Composite	Type of CB and particle size	Percolation threshold (wt %)	Electrical/thermal conductivity	Notes
CB/epoxy[5]	CPV, 30 nm	~ 25	—	Compared the elongation at break and the electrical conductivity of the composites prepared with CB, graphite, and silver-coated basalt particles
CB/epoxy[7]	Furnace CB, 3 μm	9	1.5 W m^{-1} K^{-1} at 30 wt % CB	Applicability of the composites tested for thermistors and switching voltage devices
CB/epoxy[35]	Furnace CB, 20 μm	4	—	Developed for electrical heater applications
CB/epoxy[41]	CB (1–3 nm) particles produced by shockwave technology	~ 12	1.4 S/m at 20 wt % loading	Rheology and microwave absorption properties of the studied composites
CB/silicone[42]	Acetylene black, 42 nm	~ 10	—	—
CB/silicone[43]	Acetylene black, 41 nm	—	9 S/m at ~ 40 wt %	CB imparted the highest electrical conductivity to the composites compared to copper and graphite fillers
CB/silicone[44]	CPV, 30 nm	—	3 S/m at 40 wt %	Electrical conductivity is influenced by the crosslinking density
CB/acrylonitrile butadiene rubber[45]	Fast extrusion furnace CB, 38 nm	~ 15	—	Piezoresistive effects studied for compressive strain and pressure sensor applications
CB/silicone[46]	Various types of CB	~ 25–45	—	Piezoresistivity of the composites studied

pastes have the ability to develop good contact with the mating surfaces.[20]

In the published literature, much attention has been paid to improving the dispersion of the CB in polymers and, hence, lowering the percolation threshold of CB/epoxy composites. However, there is lack of data on the effects of nanosized CBs on the thermal conductivities and mechanical properties of CB/epoxy composites. Furthermore, the research published on the CB/epoxy composites has, until now, been totally confined to those epoxy resins that are the highly crosslinked so-called glassy epoxies. These epoxies have a very high stiffness and are inherently brittle in nature. In electronic packaging applications, the high modulus of glassy epoxy-based composites do not allow internal stresses to dissipate; this results in the delamination of the epoxy from the surface.[21] Furthermore, it is not possible to produce void-free CB/glassy epoxy composites because of the difficulty of degassing these epoxies at higher loadings of filler with conventional techniques. Therefore, there is a need to replace glassy epoxies with a more compliant matrix to develop adhesives for electronic packaging applications. Rubbery epoxy (RE) and silicone elastomers could be alternatives to glassy epoxies because of their compliant nature. A RE has a glass-transition temperature below ambient temperatures and has a very low stiffness, and although it is not a true elastomer, its mechanical properties resemble one to some extent.[22,23] Furthermore, a RE has a very low viscosity before curing, fewer voids after curing, and a long workability before curing compared to a glassy epoxy. RE might be preferred over silicone for adhesive applications because of its strong adhesive nature compared to silicone. However, both RE and silicone are potential matrixes for the development of polymer composites for electronic packaging applications.

In this article, we present an investigation of the properties of CB/RE and CB/silicone composites produced by a conventional mechanical mixing (MM) technique to gauge their potential for electronic packaging applications. A range of different composites were produced as a result of variations of the following parameters: (1) type of CB, (2) loading of CB (in weight percentage), (3) silane functionalization of CB, and (4) type of matrix. The effects of varying these parameters on the electrical conductivity, thermal conductivity, and mechanical properties of the resulting composites are reported and compared.

EXPERIMENTAL

Materials

Three types of nanosized CB were used in this work: Printex XE2 (CBP), Printex 140 U (CBU; both

supplied by Evonik Industries AG, Germany), and Vulcan XC72 (CBV; Cabot Corp., USA). CBP had a reported surface area of 600 m^2/g (CTAB surface area, ASTM D 3765). CBU was a gas black with a reported BET surface area of 90 m^2/g. CBV had a BET surface area of 254 m^2/g.[24] In certain cases, the CBP particles were chemically functionalized with 3-aminopropoxyltriethoxysilane (APS) obtained from ACROS ORGANICS, (New Jeresy , USA) these are referred to as silane-functionalized carbon blacks (SCBPs) hereafter.

The RE and poly(dimethyl siloxane) (silicone elastomer) were used as matrixes for the development of composites. Epoxy resin (Epikote 862), kindly supplied by Hexion Specialty Chemicals (USA), and an aliphatic polyetheramine curing agent (Jeffamine D2000, Huntsman Corp., USA) were used in this work to produce a RE matrix. Sylgard 184 silicone elastomer, purchased from Dow Corning Ltd., USA, was used as the silicone matrix material in this study.

The RE was produced by the mixture of the epoxy resin, Epikote 862, and curing agent, Jeffamine D2000 (polypropylene oxide), at weight ratios of 25:75, respectively. We considered that the epoxy resin did, in fact, crosslink the polyetheramine oligomer (Jeffamine D2000) because the latter's content was three times higher than the former. The resulting material could, therefore, be logically termed a crosslinked polyether, but it is commonly known as a RE because it has a glass-transition temperature below normal ambient temperature[23] and a significantly lower modulus than highly crosslinked glassy epoxy.[25] The silicone elastomer was supplied as two-part liquid component kit composed of a base and a curing agent. These were mixed in a ratio of 10:1 by weight to make a silicone matrix for the composites. The base/curing agent was composed of a vinyl end-capped oligomeric dimethyl siloxane, methylhydrosiloxane as a crosslinking agent, and a platinum complex as the catalyst for the hydrosilation reaction.[26]

Composite fabrication

The CB/RE and CB/silicone composites were produced by conventional MM. To prepare the CB/RE composite samples with minimum dimensions of 40 $\times$ 25 $\times$ 10 mm^3, 40–50 g batches were prepared by the mixture of CB particles and RE resin (i.e., mixture of Epon 862 and Jeffamine D2000). All of the composite dispersions were prepared at room temperature. The CB particles were predried in an oven at 80°C for a prolonged period to remove any moisture adsorbed on their surface. The dried particles were then mixed at appropriate percentages with RE resin with a conventional mechanical mixer with a high-speed motor and a propeller attached to a shaft. This was rotated in the mixture at 1000 rpm for 30 min; these conditions were identified as optimal for achieving the highest electrical conductivities in the composites after various trials (increasing the mixing speed above 1000 rpm decreased the electrical conductivity, and increasing the mixing time had no significant effect on the electrical conductivity). After mixing, the batch was degassed *in vacuo* to remove any trapped air and poured into a custom-made aluminum mold. The filled mold was again degassed for 0.5 h to completely remove any trapped air. These composites were cured at 80°C for 2 h and 120°C for an additional 3 h. The sample of neat RE was also produced by MM.

To prepare the CB/silicone composites, CB particles were first mixed with the silicone base at 1000 rpm for 25 min. Then, the curing agent was mixed in for 5 min. The temperature of the mixture increased to 60–70°C during mixing. Therefore, the mixture was immediately cooled to 5°C by immersion in an ice bath to avoid precuring of silicone. After mixing, the batch was degassed *in vacuo* to remove any trapped air and was poured into a custom made aluminum mold. The filled mold was again degassed for 0.5 h to completely remove any trapped air. Then, curing was carried out at 90°C for 45 min.

A list of all of the fabricated composites is presented in Table II. These composites were fabricated at the maximum possible loading of various CBs.

Silane functionalization of CB

For the silane functionalization of CB particles, the CBP particles were first treated with concentrated nitric acid to produce the carboxylic and hydroxyl groups on the surface of CB. A quantity of about 15 g of CBP was added to a 6*M* solution of nitric acid. This solution was heated at about 80°C for 5 h under continuous stirring. After this, the solution was poured into distilled water to reduce its pH. CBP was filtered out and washed with distilled water to remove any remaining acid. The acid-treated CBP was dried at 60°C for 24 h and then ground with a mortar and pestle. The grafting of APS onto the CB was done in a mixture of ethanol and water (25/75 v/v) according to a procedure described in ref. [27]. To 1500 mL of the ethanol/water solution, 4.5 g of APS was added and mixed with a magnetic stirrer. Acid-treated CBP particles (ca. 15 g) were added to the ethanol/water/APS solution. This mixture was heated up to 80°C and kept at this temperature under continuous stirring for 5 h for the reaction to complete. After the completion of the reaction, the reaction product was filtered out and washed several times with distilled water. The SCBP particles

TABLE II
List of All Composites Fabricated at Various Levels of CB Loading

Composite	Type of CB	wt %	Structure of CB in the matrix
CBP/RE	CBP	2, 2.5, 3, 4, 6, 8	CBP formed chains
SCBP/RE	SCBP	8	No chains, formed very small agglomerates
CBU/RE	CBU	8, 20, 36	CBU formed small isolated agglomerates
CBV/RE	CBV	8, 12	Formed big but isolated agglomerates
CBP/silicone	CBP	6, 8	Formed chains but less extensive than those formed in RE
CBU/silicone	CBU	8	Small agglomerates widely spaced
CBV/silicone	CBV	6, 8	Large agglomerates but with fewer contacts

were dried at 50°C for 24 h and ground with a mortar and pestle.

Characterization

Transmission electron microscopy (TEM) of various CBs was performed with an FEI CM200 (Philips) field emission gun transmission electron microscope with a Gatan GIF 200 imaging filter running at 197 kV. We prepared the samples by dispersing them in methanol and then placing a drop of the dispersion on a holey carbon-coated copper grid. The morphology of the composites was observed with an LEO 1530 field emission gun scanning electron microscope. The images were obtained with secondary electrons at a primary beam energy of 3 kV with a working distance of 3 mm. Samples were prepared by the brittle fracture of liquid nitrogen cooled strips of the composites. The fractured surface of the sample was sputter-coated with a 5-nm layer of Pt/Pd alloy before scanning electron microscopy (SEM) analysis.

The thermal conductivity of the neat silicone and composites was measured (in a direction parallel to the direction of gravity in the original curing mold) by a hot disk thermal constant analyzer (Hot Disk AB, Uppsala, Sweden), which was a transient plane source technique. The sensor, which acted as both a heat source and a temperature recorder, with a radius of 3.180 mm, was sandwiched between two halves of each sample. For the measurement, each half of the sample was cut to 8–10 mm thickness, with a 20 $\times$ 20 mm^2 area, and was made into a flat surface so that a good thermal contact could be made across the contacting areas of the two pieces with the sensor. The thermal conductivity measurements were made by the application of a power of 0.1–0.2 W for between 40 and 80 s; this depended on the thermal conductivity of the sample. The thermal conductivity value was averaged from two to three measurements for each sample.

For electrical conductivity measurement, cuboid pieces of the composites ($\sim$ 6 $\times$ 6 $\times$ 2 mm^3) were placed between two copper electrodes having dimensions slightly greater than those of the sample. The electrodes were connected to a mulitmeter (Agilent 34401A, Agilent Technologies, USA), which measured the resistance of the sample with a two-probe method.[28] The samples were slightly compressed between the electrodes to ensure good contact between the sample and copper electrodes. The electrical conductivity was averaged from the measurements of five different specimens.

Compression testing of the RE, silicone, and composites was carried out on an Instron universal testing system (model no. 3382, with a 100-kN load cell, Instron, Bucks, UK). Rectangular samples ($\sim$ 8 $\times$ 8 $\times$ 10 mm^3) were compressed at a strain rate of 0.5 mm/min. A typical compression test was carried out until a crack appeared in the sample. The data were averaged by from three tested specimens of each sample.

RESULTS AND DISCUSSION

Loading of CB into the polymer resins

The composites used in this work were produced at their maximum possible loading of CB, as shown in Table II. It was found that the CBP could be loaded into the RE matrix conveniently up to a level of 6–7 wt %. At 8 wt %, this composition had such a high viscosity that it was not possible for the propeller to move in the mixture after 15 min of mixing. However, the SCBP/RE dispersion at an 8 wt % loading was easily mixed by the propeller, and the resulting dispersion was pourable. To demonstrate that SCBP reduced the viscosity of the dispersion, we measured the viscosities of the RE dispersions produced with CBP and SCBP at 4 wt % loadings. As shown in Figure 1, the viscosity of the 4 wt % SCBP/RE was significantly lower than the corresponding dispersion produced with CBP. For example, the viscosity of the 4 wt % CBP/RE was about 9 Pa s, compared to 1 Pa s at a shear rate of about 15 s^{-1}. The silane functionalization of CBP was also shown to decrease the surface area from 1012 to 746 m^2/g (the BET surface area by nitrogen gas adsorption was measured with a Quantachrome Autosorb, Florida, USA). SEM analysis [Fig. 3(c), shown later] showed that this was accompanied by a reduction in

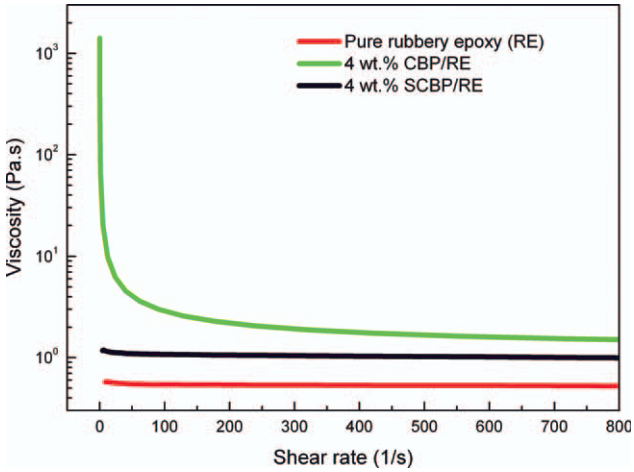

Figure 1 Viscosity versus the shear rate of the pure RE, 4 wt % CBP/RE, and 4 wt % SCBP/RE dispersions before curing as measured by a Malvern Bohlin Gemini CVOR 150 rheometer, Worcestershire, UK. [Color figure can be viewed in the online issue, which is available at wileyonlinelibrary.com.]

agglomeration, and thus, the reduction in surface area was likely due only to the surface absorption of silane, which thus decreased the interaction between the SCBP and the epoxy resin. Functionalization thus helped to increase the loading limit of CBP to 8 wt % by decreasing the viscosity of the CBP/RE dispersion.

The maximum possible loading of the different CBs depended on their surface areas. The CBP particles had the highest surface area among the CBs used. The highest surface area meant that CBP was capable of absorbing more polymer on its surface for a given weight fraction than the other CBs; this limited the maximum loading of CB to 6–7 wt %, whereas CBU had the lowest surface area and thus could be loaded up to 36 wt % into the RE.

TEM of the CB particles

TEM images of the CBs are presented in Figure 2. The CBP particles had an average size of 29 ± 5 nm. CBV had a bimodal size distribution with particles with an average size of 49 ± 5 and 19 ± 3 nm, respectively. CBU had an average particle size of 40 ± 7 nm. All of the CBs formed chains and rings. CBP and CBU formed more extended chains [Fig. 2(a,c)], whereas CBV formed chains more like rings [Fig. 2(b)]. High-resolution TEM images [Fig. 2(e,f)] revealed the turbostratic structure (i.e., lack of three-dimensional order) of the CB particles. CBP and CBV consisted of concentric onion structures formed by the repetition of carbon layers; this resulted in a columnar turbostratic pile, whereas CBU had a structure more like an isometric turbostratic pile.[29] CBU had more random and discontinuous carbon layers compared to CBP and CBV. This suggested that CBU was more amorphous in nature compared

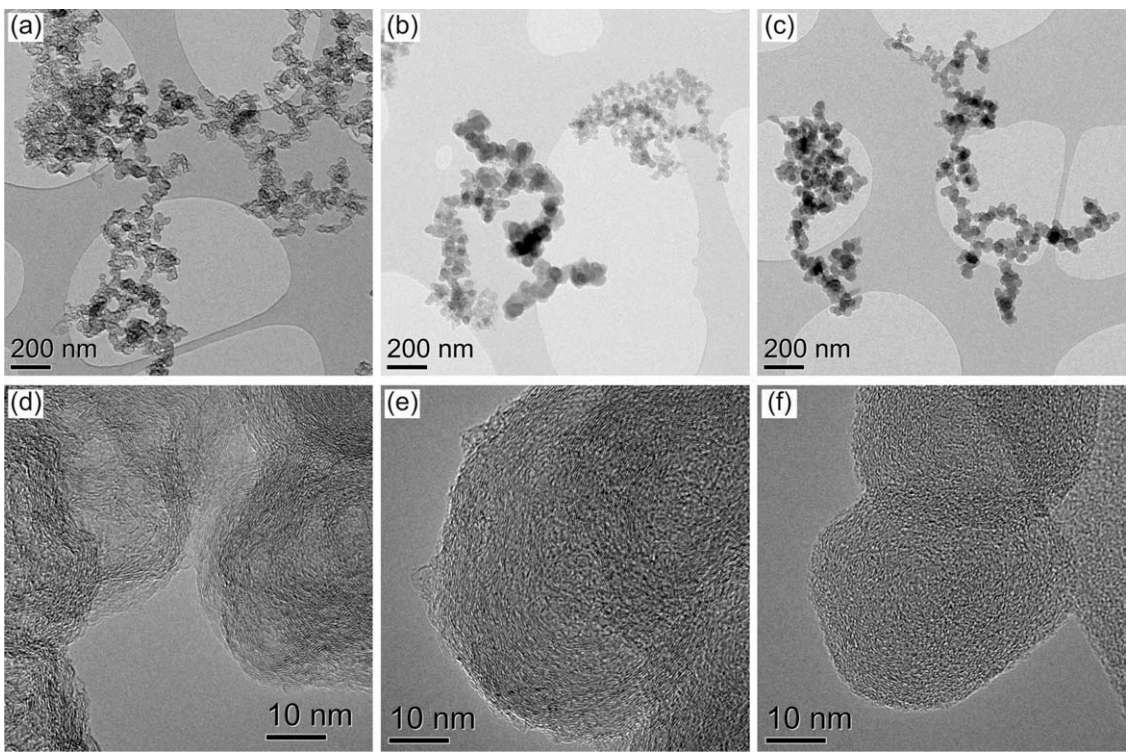

Figure 2 TEM images of (a) CBP, (b) CBV, and (c) CBU and high-resolution TEM images of (d) CBP, (e) CBV, and (f) CBU showing the turbostratic structure of CB. CBU had more random layers of carbon.

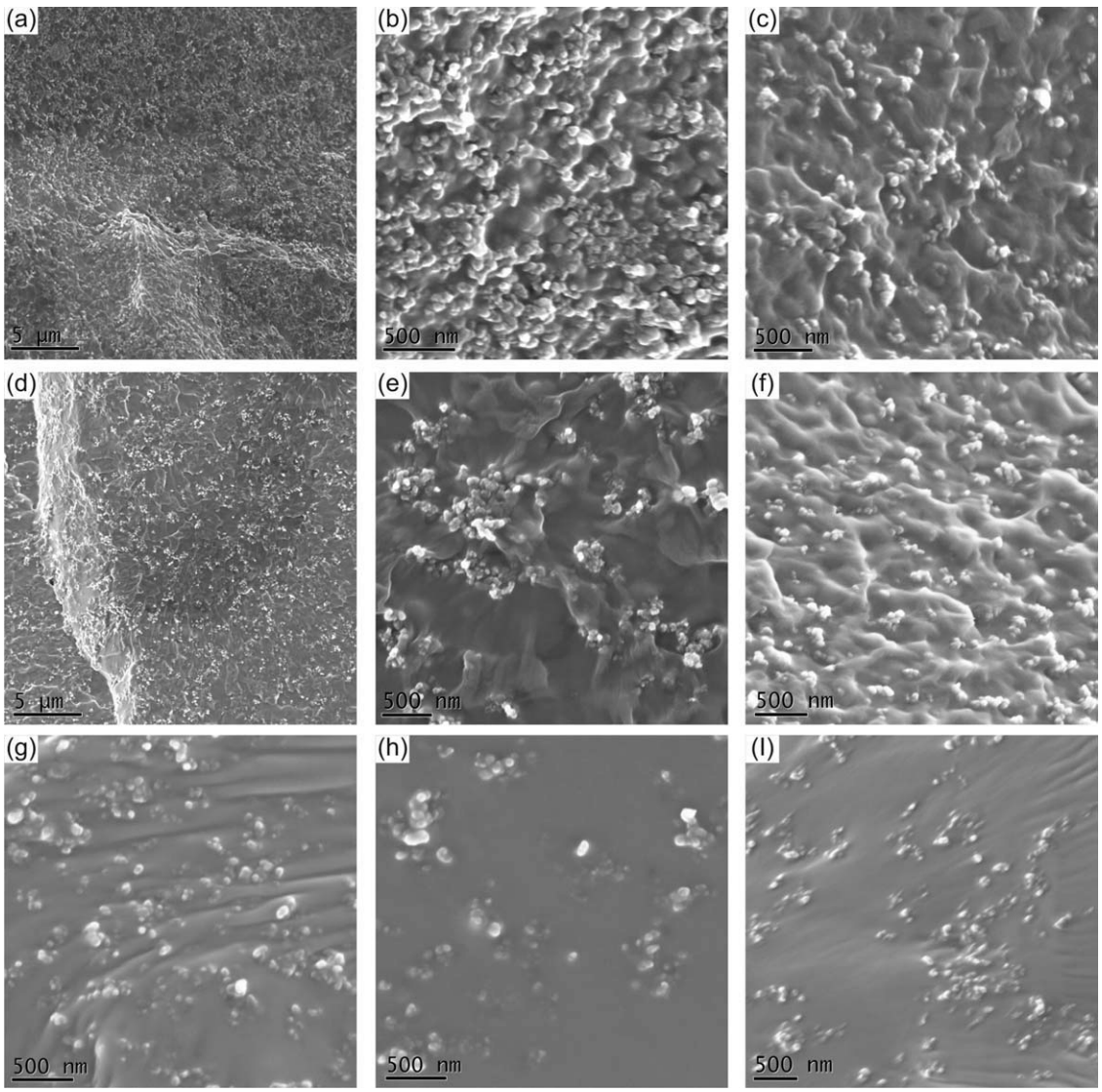

Figure 3 SEM images of (a) 6 wt % CBP/RE, (b) 8 wt % CBP/RE, (c) 8 wt % SCBP/RE, (d,e) 8 wt % CBV/RE, (f) 8 wt % CBU/RE, (g) 8 wt % CBP/silicone, (h) 8 wt % CBV silicone, and (i) 8 wt % CBU silicone composites.

to CBP and CBV, which seemed partly crystalline. Thus, in terms of graphitic character, it appeared that CBP > CBV > CBU. CBP seemed to have a more internal porosity. If open, this porosity might have contributed, in conjunction with the smaller particle size, to this material's higher surface area. CBP and CBV had rough surfaces, whereas CBU had a smooth surface. The rough surfaces were evidence for lots of edge sites (of graphene planes) at the surface, which could facilitate bonding.

Morphology of the composites

CB particles make either larger, irregular aggregates or smaller, less irregular aggregates and are called high-structure or low-structure CBs, respectively.[10] These aggregates in CBs are derived from the process of manufacturing, and we could see these features in the examination of the powders [Fig. 2(a,c)]. These aggregates could break during mixing in the resin; however, there may have remained some original aggregates, together with some reagglomeration or rearrangement of the primary particles and small aggregates. Because the resins were low-viscosity liquids, this allowed the particles to move in the resin and form agglomerates.[30] Such reagglomeration could have been influenced by the curing temperature and time.

The dispersion quality of the CB particles in the polymer matrixes is shown in the low-magnification SEM images of the composites presented in Figure 3(a,d). Overall, SEM analysis reflected that the CB particles were well dispersed and distributed in the polymer matrixes, with little evidence of large agglomerates, and these particles seemed to be connected with one another on the microscale.

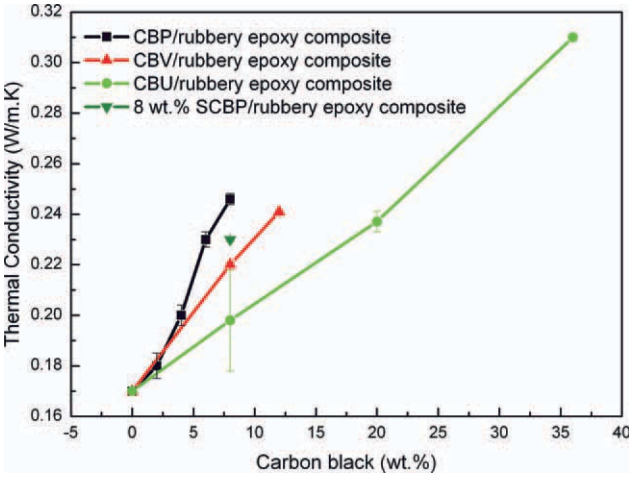

Figure 4 Thermal conductivity of the CB/RE composites as a function of the weight percentage of CB. The error bar represents the range of data points.

However, high-magnification images of the composites clearly showed that the CB particles did not exist as isolated particles in the matrix but instead formed small agglomerates with sizes of less than 200 nm (Fig. 3). These tiny agglomerates formed a certain structure (morphology) in the matrix, depending on the type of CB, as summarized in Table II. In the case of the 6 and 8 wt % CBP/RE composites [Fig. 3(a,b)], the CB particles formed large agglomerates, and these were connected with one another to form a concatenated structure (in the form of chains) running throughout the matrix. Such a structure of CBP particles in the matrix was analogous to their original structure as powders [Fig. 2(a)]. It seemed that the original structure of the CB particles (i.e., with a tendency to agglomerate) was manifested in the polymer composite. On the other hand, SCBP resulted in smaller agglomerates, and the contacts between these agglomerates were fewer, as shown in Figure 3(c). The silane functionalization might have reduced the edge sites on the surface of CBP by bonding itself on the surface. This might have reduced the ability of the CBP particles to form large agglomerates. In the case of the CBV/RE composites, although a good distribution of CBV particles in the RE could be seen [Fig. 3(d)], the population density of the CBV agglomerates appeared to be lower than that of the equivalent CBP/RE composite [Fig. 3(b)]. This showed that CBV particles had a lower structure within the composite than the CBP particles. On the other hand, the CBU particles in the CBU/RE composites had the smallest agglomerates [Fig. 3(f)], which were widely spread in the matrix. This shows that the CBU particles had the lowest structure. In general, SEM images of both the CB/RE and CB/silicone composites showed similar features. It could also be observed that in the case of the 8 wt % CBP/silicone composite [Fig. 3(g)], the CBP particles formed smaller aggregates and had lower density networks than the equivalent RE composites [Fig. 3(b)]. The RE composites had longer curing times, and this allowed the particles to diffuse in the resin and form more and bigger agglomerates compared to the silicone-based composites.

Overall, the SEM images demonstrate that CBP had the highest ability to develop a concatenated structure within the matrix. This was speculated to be due to its greater degree of graphitization (promoted agglomeration due to van der Waal's forces) and edge sites [as shown by TEM (Fig. 2)], which generated an extended chainlike structure compared to the other types of CBs. The more amorphous CBU particles had the lowest ability to form a concatenated structure in the polymer matrix.

Thermal conductivity

The thermal conductivities of the CB/RE composites produced by MM with different types of CBs as a function of the weight percentage of CB particles are presented in Figure 4 and Table III.

The thermal conductivity of the CB/RE composites for all three CBs increased approximately linearly with increasing weight percentage of CB. The

TABLE III
Compression Properties and Shore Hardness Values of the CB/RE Composites

Material	Thermal conductivity (W/m K)	Electrical conductivity (S/m)	Compressive modulus (at 10% strain; MPa)	Compressive strength at failure (MPa)	Compressive strain at failure (%)	Shore hardness (scale A)
RE	0.17	Insulating	7.39 ± 0.1	2.26 ± 0.2	26.15 ± 1.74	55.8 ± 2
2 wt % CBP/RE	0.18	$1.5 \times 10^{-7} \pm 2.7 \times 10^{-7}$	7.33 ± 0.08	4.25 ± 0.28	37.93 ± 0.38	56.8 ± 2
4 wt % CBP/RE	0.20	0.015 ± 0.005	9.25 ± 0.28	5.49 ± 0.99	37.97 ± 3.08	64.8 ± 3
6 wt % CBP/RE	0.22	0.029 ± 0.013	10.22 ± 0.01	7.25 ± 0.54	41.61 ± 1.57	64.6 ± 2
8 wt % CBP/RE	0.24	0.234 ± 0.035	11.93 ± 0.65	8.61 ± 1.84	40.45 ± 3.31	71.2 ± 4
8 wt % SCBP/RE	0.23	$6.4 \times 10^{-6} \pm 1.8 \times 10^{-6}$	10.97 ± 0.06	8.27 ± 0.06	42.37 ± 0.14	62.6 ± 5
8 wt % CBV/RE	0.22	0.002 ± 0.001	9.57 ± 0.42	4.58 ± 0.47	33.47 ± 1.12	67.9 ± 2
12 wt % CBV/RE	0.24	0.003 ± 0.001	11.75 ± 0.12	8.01 ± 0.12	38.74 ± 0.38	66.1 ± 2
8 wt % CBU/RE	0.19	Insulating	8.22 ± 0.64	5.46 ± 0.77	39.94 ± 2.02	60 ± 4
36 wt % CBU/RE	0.31	Insulating	25.53 ± 0.48	21.98 ± 5.58	33.44 ± 2.97	73 ± 2

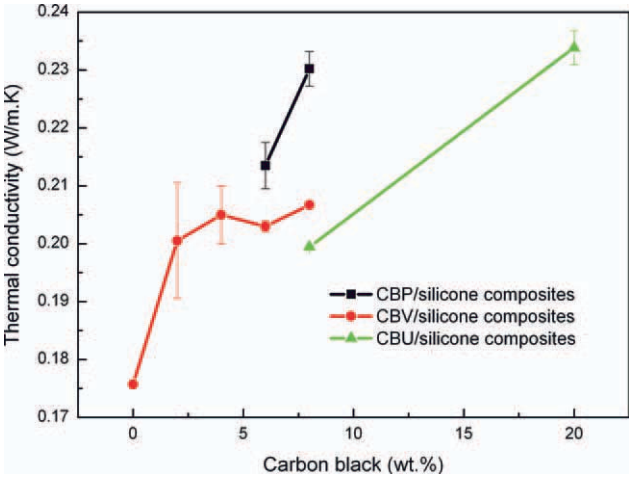

Figure 5 Thermal conductivity of the CB/silicone composites as a function of the weight percentage of CB. The effects of various types of CB on the thermal conductivity are also shown. The error bar represents the range of data points.

thermal conductivity of the CBP/RE at a maximum loading of 8 wt % CBP reached 0.24 W m^{-1} K^{-1}; this was about 40% higher than that of the RE alone (0.17 W m^{-1} K^{-1}). The thermal conductivities of the CBV/RE and CBU/RE composites at 8 wt % loading were both slightly lower than that of the 8 wt % CBP/RE composite. The highest thermal conductivity of 0.31 W m^{-1} K^{-1} was obtained from the CBU/RE composite but at 36 wt % CBU. This was still five times lower than that reported by Abdel-Aal et al.[7] for a composite produced with micrometer -sized CB particles at a loading of 30 wt %. This indicated that nanosized CB particles did not make a significant improvement in the thermal conductivity compared to micrometer-sized CB particles.

The thermal conductivities of the composites produced with CBP particles were higher than those of the composites containing other types of CBs at equivalent loadings of 8 wt %. The highest thermal conductivity of CBP/RE was attributed not only to the more graphitic nature of CBP [Fig. 2(d)][31] but also to its concatenated structure in the RE matrix, as observed by SEM, which led to the formation of more effective conducting networks within the matrix. The data showed that a high CB structure in the matrix could promote the transport of heat efficiently within the matrix.

The thermal conductivity of the composite produced with SCBP at an 8 wt % loading was 4% lower than the corresponding composite containing unfunctionalized CB. This was attributed to the formation of smaller aggregates and a less concatenated structure of SCBP in the matrix [Fig. 3(c)], which reduced the efficiency of the thermally conducting networks.

The thermal conductivities of the CB/silicone composite as a function of the weight percentage of CB are presented in Figure 5 and Table IV.

Similar to the thermal conduction behavior of the CBP/RE composite, the CBP/silicone composite at 8 wt % loading had the highest thermal conductivity (0.23 W m^{-1} K^{-1}) compared to the equivalent CBV/silicone or CBU/silicone composites. This was 35% higher than the neat silicone alone (0.17 W m^{-1} K^{-1}) and 4% lower than the equivalent CBP/RE composite. The thermal conductivity of the CBU/silicone composite produced at 20 wt % loading reached 0.23 W m^{-1} K^{-1}.

Lin and Chung[32] reported the thermal conductivity of CBV-based thermal paste to be 0.149 W m^{-1} K^{-1} (as measured by the steady-state method) at about 10 wt % CBV. Compared with this, the CBV/RE and CBV/silicone composites developed in this study at 2 wt % lower loadings of CBV had about 47 and 38% higher thermal conductivities, respectively, than the CBV-paste.

The maximum thermal conductivity obtained for the CBP/RE and CBP/silicone composites at 8 wt % loading were 0.24 and 0.23 W m^{-1} K^{-1}, respectively. CB particles made no significant improvements in the thermal conductivity of the RE or silicone polymer compared to other carbon nanofillers, such as carbon nanotubes, carbon nanofibers, and graphite nanoplatelets,[27,31,33,34] which have been reported to produce substantial improvements in the thermal conductivity of the polymers. Primarily, the turbostratic structure (the absence of a long-range order)[29] of the CB particles was responsible for the low

TABLE IV
Compression Properties and Shore Hardness Values of the CB/Silicone Composites

Material	Thermal conductivity (W/m K)	Electrical conductivity (S/m)	Compressive modulus (at 10% strain; MPa)	Compressive strength at failure (MPa)	Compressive strain at failure (%)	Shore hardness (scale A)
Silicone (sil)	0.17	Insulating	5.57 ± 0.45	41.47 ± 6	62.51 ± 1.44	53.0 ± 1.0
6 wt % CBP/sil	0.21	Insulating	6.05 ± 0.28	46.97 ± 15.08	60.14 ± 7.33	56.2 ± 1.8
8 wt % CBP/sil	0.23	0.012 ± 0.002	7.07 ± 0.29	85.67 ± 17.24	71.91 ± 1	56.4 ± 0.9
6 wt % CBV/sil	0.20	Insulating	4.6 ± 0.11	31.14 ± 2.78	56.28 ± 0.25	51.1 ± 1.9
8 wt % CBV/sil	0.21	Insulating	5.45 ± 0.17	29.91 ± 0.96	55.92 ± 0.47	53.0 ± 1.8
8 wt % CBU/sil	0.19	Insulating	5.32 ± 0.05	55.46 ± 3.21	65.87 ± 1.03	52.0 ± 1.6

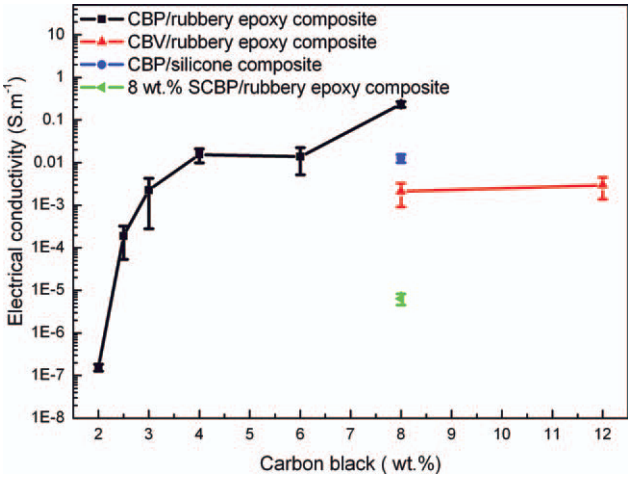

Figure 6 Electrical conductivity versus the weight percentage of CB particles of the CBP/RE and CBV/RE composites.

thermal conductivity of the composites. However, another factor could have been the size of the CB nanoparticles and their propensity to form aggregates. Such aggregates consisting of nanoparticles could result in increased thermal contact resistance within and between the aggregates and could result in an increased scattering of phonons.

Electrical conductivity

The electrical conductivity as a function of the weight percentage of CB for the CBP/RE and CBV/RE composites is presented in Figure 6 and Table III. The electrical conductivity of the 8 wt % CBP/silicone composite is also shown in Figure 6 and Table IV.

The electrical conductivities of the CBP/RE composites increased as a function of the weight percentage of CBP. The electrical resistivity of the pure RE in the cured state was very high, and its exact value was not determined because of a limitation of the instrument, which only had a detectable range up to 100 MΩ. As shown in Figure 6, the electrical conductivity of the CBP/RE increased sharply with an increase in the CBP content of up to 2.5 wt %. This showed that the composite underwent the transition from an insulator to a conductor. This rapid increase in the electrical conductivity of the composite was attributed to the ability of the CBP particles to make conductive networks throughout the matrix. The electrical conductivities of the CBP/RE composites, although improved significantly compared to the RE alone, were not high enough for these composites to be used as electrically conductive adhesives. However, these composites may be suitable for applications in fields like electromagnetic interference shielding, electrostatic dissipation, electrical heaters, and thermistors.

It can be seen from Figure 6 that the percolation threshold for the CBP/RE composite was found to be about 2.25 wt % (1.04 vol %) of CBP loading according to the definition stated in the Introduction. The percolation threshold values reported in this work for the CBP/RE composites were significantly lower than those reported in the literature.[5,16,35] The electrical conductivity of the composites depended on the ability of the fillers to form conductive networks. The electrical conductivity of such a system above the percolation limit depends on electron tunneling due to the small interparticle distance and can be described with a bond-percolation-like power law according to following equation:[18,36]

$$\sigma \propto (\phi - \phi_c)^t \qquad ()$$

where σ is the electrical conductivity of the composite, ϕ is the volume fraction of the filler, ϕ_c is the volume fraction of the filler at the percolation threshold, and t is the critical exponent. A universal value of $t = 2$ was reported for high-structure CBs composites.[37] Figure 7 shows the linear fitting of the electrical conductivity data according to Eq. (1). A reasonable fit for log σ versus log($\phi - \phi_c$) with a slope of $t \approx 2$ was obtained. This was in good agreement with the percolation theory, which predicts a value of $t = 2$, and several groups measured the same value for various disordered conductor–insulator composites.[38,39]

The electrical conductivity of the CBV/RE composite at 8 wt % loading of CBV was 0.002 S/m (Fig. 6); this was two orders of magnitude lower than that of the corresponding composite produced with 8 wt % CBP. The electrical conductivity of the CBV/RE

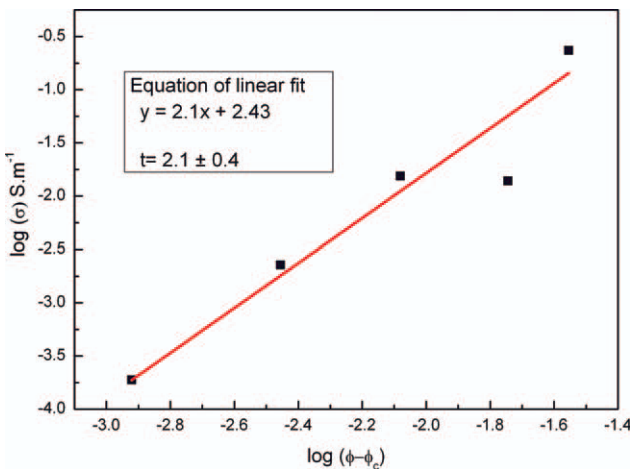

Figure 7 Linear fitting of the electrical conductivity data of the CBP/RE composite to the bond-percolation equation.

composite did not increase further with increasing CBV loading. Thus, the electrical conductivity data of the CBV/RE composites showed that the percolation threshold of these composites was lower than 8 wt %. This was significantly lower than the 25 wt % reported by Novak et al.[5] for CBV/epoxy composites produced with a similar CB to that used here for the fabrication of CBV/RE composites. This significantly lower percolation threshold might have been due to the improved dispersion and distribution of CBV in the RE achieved by MM. The significantly lower viscosity of the RE compared to that of conventional glassy epoxies might have been useful in effectively dispersing the CB and in developing conducting networks.

The electrical conductivity data indicated the superiority of CBP over CBV in improving the electrical conductivity of the composites; this was related to the high structure of CBP, which resulted in the concatenated structure within the matrix and led to the formation of more effective conducting networks. The CBP particles could produce electrically conducting composites at lower loadings than CBV. On the other hand, the CBU/RE composites were found to be electrically insulating, even at a loading of 36 wt % CB. This was attributed to a lack of chainlike structure in CBU compared to CBP and CBV [Fig. 3(f)]. Similarly, SCBP (8 wt % SCBP/RE) produced an electrically insulating composite by breaking the continuity of the conducting networks.

In the case of the CB/silicone composites, the composites produced with CBV and CBU at all loadings were electrically insulating. The CBP/silicone composite produced at 8 wt % loading was electrically conducting. However, it had an order of magnitude lower electrical conductivity than the equivalent RE composite. Because the CBP/silicone at 6 wt % loading was electrically insulating, we deduced that the CBP/silicone composites had a percolation threshold between 6 and 8 wt %. The significantly higher percolation threshold of the CBP/silicone composite compared to that of the CBP/RE composite suggested that the nature of the matrix played a vital part in the electrical conduction of the filled polymer composites. In the case of the CBV/silicone and CBU/silicone composites, in addition to the high electrical insulation of the silicone matrix, the aggregates of CBV and CBU were significantly spaced out from one another, with large amounts of silicone matrix between so that these aggregates were not able to form contact with one another, as observed by SEM [Fig. 3(h,i)]. These factors might have been the reasons for the highly electrically insulating nature of the CBV/silicone and CBU/silicone composites.

Although there was a strong difference in the electrical conductivity of the composites with different CB particles, the thermal conductivity of these composites was very similar at equivalent loadings and were not influenced by the structure of CB in the matrix and the nature of the matrix. The electrical conductivity results clearly demonstrate that the electrical conductivity of the CB-based composites depended on the ability of CB to form a concatenated structure and on the electrical resistivity of the matrix. Thus, these results show that it is possible to make an electrically conducting or insulating composite with different types of CB particles without significantly impairing the thermal conductivity of these composites. Composites with these attributes are of great interest for electronic packaging applications.

Compression testing

The compression properties and Shore hardness values of the neat RE, silicone, CB/RE composites, and CB/silicone composites are presented in Tables III and IV, respectively.

The RE had a low modulus, which showed its compliant nature. CB addition to the RE increased the compressive properties of the RE with increasing CB content. As shown in Table III, 8 wt % CBP increased the compressive modulus, strength, and strain to failure of the RE by about 1.6, 4, and 1.5 times, respectively. SCBP reduced the modulus of the composite slightly without making an appreciable change in the compressive strength compared to the equivalent composite produced with CBP. On the other hand, although CBV and CBU increased the compressive modulus of the RE, their corresponding composites at 8 wt % loading had about a 1.5 times lower compressive strength than the equivalent CBP/RE composite. This was attributed to the fewer contacts between the CB aggregates in these composites, as observed by SEM (Fig. 3). The CBU/RE composite at 36 wt % loading produced increases of about 3 and 10 times in the compressive modulus and strength of the RE, respectively.

The compressive properties of the CB/silicone composites also increased with increasing CB loading. In the case of the 8 wt % CBP/silicone composite, the compressive modulus of silicone was increased by 1.26 times. This was 1.68 times lower than that of the equivalent CBP/RE composite, and this suggested that the CBP/silicone composites were more compliant materials than the CB/RE composites. CBP increased the compressive strength of the silicone, but the standard deviations were significantly large. This indicated that CBP might have had nonuniform distribution in the silicone matrix. On the other hand, neither CBV and CBU changed the compressive modulus of silicone at 8 wt % loading. This behavior might have been due to the more

isolated aggregates of CB in the silicone matrix, as observed by SEM (Fig. 3). CBU increased the compressive strength of silicone, but CBV significantly reduced the compressive strength of the silicone at 8 wt % loading. It is known that functional groups on the surface of CB play an important role in building stronger bonding between the polymer matrix and the CB particles.[40] Such stronger bonds lead to an improvement in the mechanical properties of the polymers.[40] Therefore, it might be possible that the interaction between the CBV and silicone polymer was not strong because of the presence of fewer functional groups on the surface of CBV, which resulted in a lower compressive strength of the CBV/silicone composites compared to those of the the composites produced with other CBs.

The Shore hardness values of the CB/RE and CB/silicone composites are also presented in Tables III and IV, respectively. Similar to the compression properties, the Shore hardness values of CB/RE composites increased with increasing CB content. A maximum value of 71 was measured for the 8 wt % CBP/RE composites. This was about a 28% increase over that of the RE alone. Similar to the compression properties, at an equivalent loading, CBP produced composites with higher Shore hardness values compared with CBV and CBU. CBP also slightly increased the Shore hardness of silicone at an 8 wt % loading. However, both CBV and CBU made no significant changes to the Shore hardness of silicone at an 8 wt % loading.

CONCLUSIONS

Three different types of nanosized CBs were dispersed in two compliant rubbery matrixes, RE and silicone, to produce a range of composites. The effects of loading and type of CB on the morphology, thermal conductivity, electrical conductivity, compression, and Shore hardness of the composites were investigated. The CB particles formed aggregates, which were connected to one another to form a concatenated structure in the matrix. CBP had the strongest ability to form a concatenated structure because of its high surface area compared to those of CBV and CBU. Such a concatenated structure resulted in high electrical conductivities in the composites, but its effect on the thermal conductivity was not significant. The lowest percolation threshold, about 2.2 wt %, was obtained for the CBP/RE composites; this was considerably lower than those reported for CB/epoxy composites in the literature and was attributed to the high structure and good dispersion of the CBP particles. It was possible to produce electrically insulating or conducting composites with CBU and CBP, respectively, without impairing the thermal conductivities of the composites. None of the CB particles produced substantial increases in the thermal conductivities of the composites; this might have been due to their turbostratic structure and their presence as nanosized particles that offered higher resistance to phonon transport. The nature of the matrix had no significant effect on the thermal conductivities of the CB/polymer composites, but it had a strong impact on the electrical conductivities of the composites. The CBP/silicone composites had lower electrical conductivities compared to the CBP/RE composites but similar thermal conductivities.

Compression and Shore hardness testing showed that both the compressive modulus and strength and the Shore hardness values of the RE increased with increasing CBP content. All types of CB particles significantly improved the compressive strength of the RE without significantly increasing its stiffness. As for the transport properties, this increase was most noticeable with CBP. In the case of the CB/silicone composites, a greater improvement in the mechanical properties was again produced by CBP compared to CBV and CBU. However, neither CBU nor CBV increased the compressive modulus of silicone at an 8 wt % loading because of presence of isolated aggregates in the silicone matrix. The CB/silicone composites were more compliant than the CB/RE composites. Nevertheless, the CB/RE composites, because of their high adhesive nature, could be promising alternatives to glassy epoxy based adhesives for use in electronic packaging applications.

The authors thank Morgan AM&T and Engineering and Physical Sciences Research Council for funding a Dorothy Hodgkin Postgraduate Award Scholarship (M. A. Raza's).

References

1. Li, Y.; Wong, C. P. Mater Sci Eng Rep 2006, 51, 1.
2. D.D.L, C., Carbon 2001, 39, 279.
3. Feller, J. F.; Chauvelon, P.; Linossier, I.; Glouannec, P. Polym Test 2003, 22, 831.
4. Xie, S.-H.; Zhu, B.-K.; Xu, Z.-K.; Xu, Y.-Y. Mater Lett 2005, 59, 2403.
5. Novak, I.; Krupa, I.; Chodak, I. Eur Polym J 2003, 39, 585.
6. Li, Y.; Wang, S.; Zhang, Y.; Zhang, Y. J Appl Polym Sci 2005, 98, 1142.
7. Abdel-Aal, N.; El-Tantawy, F.; Al-Hajry, A.; Bououdina, M. Polym Compos 2008, 29, 511.
8. Feller, J. F.; Linossier, I.; Grohens, Y. Mater Lett 2002, 57, 64.
9. Bloor, D.; Donnelly, K.; Hands, P. J.; Laughlin, P.; Lussey, D. J Phys D: Appl Phys 2005, 38, 2851.
10. Marsh, H.; Heintz, E. A.; Rodriguez-Reinoso, F. Introduction to carbon technologies, Uniersidad de Alicante, Secretariado de Publicaciones: Alicante, Spain, 1997.
11. Fukahori, Y. J Appl Polym Sci 2005, 95, 60.
12. Çopuroĝlu, M.; Şen, M. Polym Adv Technol 2005, 16, 61.
13. Horrocks, A. R.; Mwila, J.; Miraftab, M.; Liu, M.; Chohan, S. S. Polym Degrad Stab 1999, 65, 25.
14. Liou, W.-J.; Lin, H.-M. China Particuol 2007, 5, 225.

15. Manickam, M.; Takata, M. J Power Sources 2002, 112, 116.
16. Zhang, W.; Blackburn, R. S.; Dehghani-Sanij, A. A. J Mater Sci 2007, 42, 7861.
17. Sumfleth, J.; Buschhorn, S.; Schulte, K. J Mater Sci 2011, 46, 659.
18. Stankovich, S.; Dikin, D. A.; Dommett, G. H. B.; Kohlhaas, K. M.; Zimney, E. J.; Stach, E. A.; Piner, R. D.; Nguyen, S. T.; Ruoff, R. S. Nature 2006, 442, 282.
19. Bauhofer, W.; Kovacs, J. Z. Compos Sci Technol 2009, 69, 1486.
20. Leong, C.-K.; Aoyagi, Y.; Chung, D. D. L. J Electron Mater 2005, 34, 1336.
21. Prasher, R. S. IEEE Trans Components Packaging Technol 2004, 27, 702.
22. Gauthier, C.; Chazeau, L.; Prasse, T.; Cavaille, J. Y. Compos Sci Technol 2005, 65, 335.
23. Liu, L.; Wagner, H. D. Compos Sci Technol 2005, 65, 1861.
24. Leong, C.-K.; Aoyagi, Y.; Chung, D. D. L. Carbon 2006, 44, 435.
25. Raza, M. A.; Westwood, A. V. K.; Stirling, C. Mater Chem Phys, 2012, 132, 63.
26. Efimenko, K.; Wallace, W. E.; Genze, J. J Colloid Interface Sci 2002, 254, 306.
27. Ganguli, S.; Roy, A. K.; Anderson, D. P. Carbon 2008, 46, 806.
28. Luheng, W.; Tianhuai, D.; Peng, W. Carbon 2009, 47, 3151.
29. Sciences of Carbon Materials; Marsh, H.; Rinoso, F. R., Eds.; Publicaciones Universidad de Alicante: Alicante, Spain, 1997.
30. Schueler, R.; Petermann, J.; Schulte, K.; Wentzel, H.-P. J Appl Polym Sci 1997, 63, 1741.
31. Gojny, F. H.; Wichmann, M. H. G.; Fiedler, B.; Kinloch, I. A.; Bauhofer, W.; Windle, A. H.; Schulte, K. Polymer 2006, 47, 2036.
32. Lin, C.; Chung, D. D. L. Carbon 2009, 47, 295.
33. Raza, M. A.; Westwood, A. V. K.; Stirling, C.; Hondow, N. Compos A 2011, 42, 1335.
34. Raza, M. A.; Westwood, A.; Brown, A.; Hondow, N.; Stirling, C. Carbon 2011, 49, 4269.
35. El-Tantawy, F.; Kamada, K.; Ohnabe, H. Mater Lett 2002, 56, 112.
36. Yuen, S.-M.; Ma, C.-C. M.; Wu, H.-H.; Kuan, H.-C.; Chen, W.-J.; Liao, S.-H.; Hsu, C.-W.; Wu, H.-L. J Appl Polym Sci 2007, 13, 1272.
37. Balberg, I. Carbon 2008, 40, 139.
38. Heaney, M. B. Phys Rev B 1995, 52, 12477.
39. Carmona, F. Phys A 1989, 157, 461.
40. Zhang, Y.; Pang, M.; Xu, Q.; Lu, H.; Zhang, J.; Feng, S. Polym Eng Sci 2011, 51, 170.
41. Kotsilkova, R.; Nesheva, D.; Nedkov, I.; Krusteva, E.; Stavrev, S. J App Polym Sci 2004, 92, 2220.
42. Sau, K. P.; Khastgir, D.; Chaki, T. K. Die Angewandte Makromolekulare Chemie 1998, 258, 11.
43. Princy, K. G.; Joseph, R.; Kartha, C. S. J App Polym Sci 1998, 69, 1043.
44. Zhang, J.; Feng, S. J App Polym Sci 2003, 89, 3471.
45. Mahmoud, W. E.; El-Lawindy, A. M. Y.; Eraki, M. H. E.; Hassan, H. H. Sensors and Actuators A 2007, 136, 229.
46. Wang, P.; Ding, T. J App Polym Sci, 2010, 116, 2035.